

PAPER • OPEN ACCESS

The spatially anisotropic triangular lattice antiferromagnet: Popov-Fedotov method

To cite this article: Pham Thi Thanh Nga *et al* 2017 *J. Phys.: Conf. Ser.* **865** 012014

View the [article online](#) for updates and enhancements.

Related content

- [Physical properties in the cluster-based magnetic-diluted triangular lattice antiferromagnets \$\text{Li}_2\text{Sc}_{1-x}\text{Sn}_x\text{Mo}_3\text{O}_8\$](#)
Yuya Haraguchi, Chishiro Michioka, Hiroaki Ueda *et al.*
- [Effects of magnetic field and hydrostatic pressure on the distorted triangular lattice antiferromagnet \$\text{RbFeBr}_3\$](#)
Nobuyuki Kurita and Hidekazu Tanaka
- [Spin-gap observation in the triangular lattice antiferromagnet \$\text{InMnO}_3\$ by high-field ESR](#)
H Ohta, N Matsumi, S Okubo *et al.*

The spatially anisotropic triangular lattice antiferromagnet: Popov-Fedotov method

Pham Thi Thanh Nga¹, Phan Thu Trang² and Nguyen Toan Thang³

¹ Thuyloi University, 175 Tay Son, Hanoi, Vietnam

² Hanoi National University of Education, 136 Xuan Thuy, Hanoi, Vietnam

³ Institute of Physics, 10 Dao Tan, Hanoi, Vietnam

E-mail: nga_ptt@tlu.edu.vn

Abstract. We present an analysis of the antiferromagnetic Heisenberg model on an triangular lattice with spatially anisotropic J_1 - J_2 exchange interactions. We apply the Popov-Fedotov method based on introducing an imaginary valued chemical potential to enforce the auxiliary fermion constraint exactly. The staggered magnetization, magnon spectra, free energy are computed in one loop approximation and compared using two different constraints: exact and on average. In the limit of zero temperature the results are identical, whereas at higher temperature significant differences are found. The comparisons with the results obtained by other methods are discussed.

1. Introduction

Frustrated quantum antiferromagnets have been much studied in recent years. One of the challenges is to understanding the interplay between quantum fluctuations and frustration [1, 2]. In this context, the triangular lattice Heisenberg antiferromagnet is a such magnet. The isotropic $S = 1/2$ quantum Heisenberg antiferromagnet (*HAF*) on the triangular lattice has been studied for the last few decades by analytical [3, 4] as well as numerical [5 - 7] methods. It is widely believed that the classical noncollinear 120° spin structure is stable in the quantum case with the strong reduction of staggered moment [4]. However, there exists no good material candidate for the pure isotropic triangular lattice *HAF*. The real magnets have considerable spatially in-plane anisotropies [8], in particular for Cs_2CuCl_4 [9, 10] and Cs_2CuBr_4 [10, 11] compounds. There are several analytical [12-15] and numerical [16, 17] investigations of the anisotropic triangular model.

The goal of this report is to study the spin $S = 1/2$ Heisenberg antiferromagnet on anisotropic triangular lattice, applying Popov-Fedotov formalism [18] for the semi-fermionic spin representation. The use of different representations of the spin operators in terms of the auxiliary Fermi or Bose operators is one basic approach to the investigation of spin systems. However, the representation of spins as the bilinear canonical operators enlarges the dimensionality of Hilbert space in which these operators are acting. Thus, one must impose the constraint on the auxiliary operators to remove the unphysical states from the consideration. The simplest way to cure the constraint problem is the replacement of the local by a so-called global constraint, where the number of auxiliary particles is fixed only in the average over all sites. Popov-Fedotov proposed a new method when the local constraint is taken into account exactly by introducing



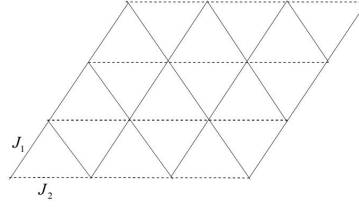


Figure 1. Anisotropic triangular lattice

the proper imaginary chemical potential for spin $S = 1/2$ and $S = 1$. Later, Veits et al have extended the Popov-Fedotov trick for arbitrary spin [19]. The Popov-Fedotov formalism then has been applied for the various spin-1/2 Heisenberg models [20-25].

In this paper we study the Heisenberg antiferromagnet on an anisotropic triangular lattice, following closely the calculations carried out in [25]. The plan of the paper is the following. In section II, we introduce the model and the classical phases. In the section III, we present the results for the sublattice magnetization, the free energy and the specific heat. In the last section we shall conclude with our results.

2. Model and classical state

The Hamiltonian of the Heisenberg antiferromagnet on an anisotropic triangular lattice is written as:

$$H = J_1 \sum_i \sum_{j=i+\vec{\delta}_{2,3}} \vec{S}_i \cdot \vec{S}_j + J_2 \sum_i \sum_{k=i+\vec{\delta}_1} \vec{S}_i \cdot \vec{S}_k \quad (1)$$

where \vec{S}_i denotes the $S = 1$ spin vector operator. The first sum runs over all nearest - neighbour pair along the x -axis with the antiferromagnetic exchange interaction J_1 ($J_1 > 0$) and the second sum runs over all other nearest neighbour pairs (See Fig 1.) with the interaction J_2 ($J_2 > 0$).

The nearest-neighbour bond vectors are given by:

$$\vec{\delta}_1 = a(1, 0); \vec{\delta}_2 = a \left(-\frac{1}{2}, \frac{\sqrt{3}}{2} \right); \vec{\delta}_3 = a \left(\frac{1}{2}, \frac{\sqrt{3}}{2} \right) \quad (2)$$

The bonds J_1 and J_2 are competing interactions and lead to magnetic frustration. Note that in the limit $J_1 = 0$ the model reduces to decoupled chains, the limit $J_1 = J_2$ corresponds to the isotropic triangular lattice, while in the case $J_2 = 0$ the model becomes topologically equivalent to the square lattice. In two dimensional frustrated lattice described by Hamiltonian (1) the classical ground states have long range order, which are the collinear ordering and the spiral ordering [1, 2]. Both orderings are obtained in the following.

In the classical limit of $S = \infty$, we assume that the spins are planar in the plane Oxz and are described by some magnetic ordering vector \vec{Q} as follows:

$$\vec{S}_i = S \left(\vec{u} \sin \vec{Q} \vec{r}_i + \vec{v} \cos \vec{Q} \vec{r}_i \right) \quad (3)$$

where \vec{u}, \vec{v} are two orthonormal unit vectors in the plane Oxz . The vector \vec{Q} defines the relative orientation of the spins on the lattice, namely an angle between the vectors \vec{S}_i and \vec{S}_j is given by:

$$\theta_{ij} = \theta_i - \theta_j = \vec{Q} \cdot (\vec{r}_i - \vec{r}_j) \quad (4)$$

Inserting \vec{S}_i into Hamiltonian (1) we get the classical energy in terms of the ordering vector \vec{Q} as follows:

$$E_{cl} = \frac{1}{2} N S^2 J(\vec{Q}) \quad (5)$$

where N is site number of the lattice and $J(\vec{Q})$ is the Fourier transform of the exchange integral:

$$J(\vec{Q}) = \sum_{\vec{\delta}_1} J_{\vec{\delta}_1} \cos(\vec{Q}\vec{\delta}_1) = 2J_1 \left(\alpha \cos Q_x + 2 \cos \frac{Q_x}{2} \cos \frac{\sqrt{3}}{2} Q_y \right) \quad (6)$$

where $\alpha = \frac{J_2}{J_1}$ and we let the lattice $a = 1$.

By minimizing the classical energy (5) with respect to the vector \vec{Q} , we find two kinds ordered phases:

i) Collinear Neel state is characterized by $\vec{Q} = \left(0, \frac{2\pi}{\sqrt{3}}\right)$ for the region $0 \leq \alpha \leq \frac{1}{2}$.

ii) Incommensurate spiral state with $\vec{Q} = \left(2\cos^{-1}\left(-\frac{1}{2\alpha}\right), 0\right)$, where $\theta = \arccos\left(-\frac{1}{2\alpha}\right)$. For $\alpha = 1$ we have a triangular lattice which corresponds to the 120° spin structure.

In the following we study the influence of the fluctuations on the classical state by means of Popov-Fedotov functional integral method, applying the calculations done in [25].

3. The results

3.1. Mean-field approximation

Working in the local coordinate system and parametrizing the classical state by ordering vector, one is able to express in a unique form the results for both the Neel and the spiral state. We introduce notations for $\lambda, \gamma_x(\vec{p}), \gamma_y(\vec{p}), \gamma_\omega(\vec{p})$:

a) For Neel state: $0 \leq \alpha \leq \frac{1}{2}$,

$$\lambda = 2(2 - \alpha)J_1 \quad (7)$$

$$\begin{cases} \gamma_x(\vec{p}) = \frac{1}{\alpha-2} \left(\alpha \cos p_x - 2 \cos \frac{p_x}{2} \cos \frac{\sqrt{3}}{2} p_y \right) \\ \gamma_y(\vec{p}) = \frac{1}{\alpha-2} \left(\alpha \cos p_x + 2 \cos \frac{p_x}{2} \cos \frac{\sqrt{3}}{2} p_y \right) \\ \gamma_\omega(\vec{p}) = 0 \end{cases} \quad (8)$$

b) For the spiral state: $\alpha > \frac{1}{2}$,

$$\lambda = 2J_1 \left(\alpha + \frac{1}{2\alpha} \right) = \frac{J_1}{\alpha} (2\alpha^2 + 1) \quad (9)$$

$$\begin{cases} \gamma_x(\vec{p}) = \frac{1}{2\alpha^2+1} \left[(2\alpha^2 - 1) \cos p_x + 2 \cos \frac{p_x}{2} \cos \frac{\sqrt{3}}{2} p_y \right] \\ \gamma_y(\vec{p}) = -\frac{2\alpha}{2\alpha^2+1} \left(\alpha \cos p_x + 2 \cos \frac{p_x}{2} \cos \frac{\sqrt{3}}{2} p_y \right) \\ \gamma_\omega(\vec{p}) = -\frac{\sqrt{4\alpha^2-1}}{2\alpha^2+1} \left(\sin p_x - 2 \sin \frac{p_x}{2} \cos \frac{\sqrt{3}}{2} p_y \right) \end{cases} \quad (10)$$

The sublattice magnetization per site in the mean field approximation reads:

$$m_o = \frac{1}{2} \tanh(\beta \lambda m_o) \quad (11)$$

In the case of average constraint, instead of equation (11) one has:

$$\tilde{m}_o = \frac{1}{2} \tanh\left(\frac{\beta \lambda \tilde{m}_o}{2}\right) \quad (12)$$

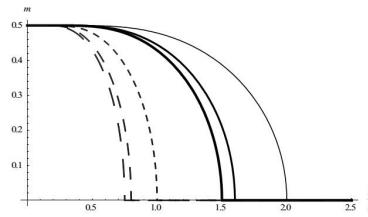


Figure 2. Temperature dependence of mean field magnetization m_o (for exact constraint: full line, from right to left) and \tilde{m}_o (for: average constraint: dashed line, from right to left) for Neel state with $\alpha = 0, \alpha = 0.4, \alpha = 0.5$.

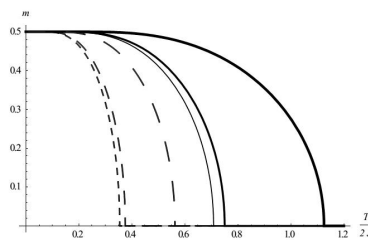


Figure 3. Temperature dependence of mean field magnetization m_o (for exact constraint: full line, from left to right) and \tilde{m}_o (for: average constraint: dashed line, from left to right) for incommensurate spiral phase with $\alpha = 0.75, \alpha = 1, \alpha = 2$.

Accordingly, the equations result in different critical temperature:

$$\begin{aligned} \text{exact-constraint : } T_C &= \frac{\lambda}{2} \\ \text{average-constraint : } T_{Co} &= \frac{\lambda}{4} \end{aligned} \quad (13)$$

From (13) we see the critical temperature for the case of exact constraint is higher than for average constraint is higher than for average constraint $\frac{T_C}{T_{Co}} = 2$. This is due to thermal fluctuations into unphysical spinless states when constraint is treated globally, which reduce the magnetic moment. However, at zero temperature both constraint methods give the same result. In Fig 2 and Fig 3 we plot the temperature dependence of the mean field sublattice magnetization for Neel and Spiral states, respectively. Fig 2 and Fig 3 show the difference of the results for the case of exact constraint and average one.

The mean field free energy per site can be expressed in term of the magnetization m_o as follows:

$$\frac{F_{MF}}{N} = \frac{1}{2}\lambda m_o^2 - \frac{1}{\beta} \ln \left(2 \cosh \frac{\beta \lambda m_o}{2} \right) \quad (14)$$

In the case of average projection instead of (14) one has:

$$\frac{F_{MF}}{N} = \frac{1}{2}\lambda \tilde{m}_o^2 - \frac{2}{\beta} \ln \left(2 \cosh \frac{\beta \lambda \tilde{m}_o}{2} \right) \quad (15)$$

Again, at $T = 0K$, the Eqs. (14) and (15) lead to the same result.

3.2. Fluctuation contributions

In one loop approximation we obtain the fluctuation contributions to the longitudinal δm_{zz} and transverse δm_{+-} parts for the magnetization as follows:

$$\delta m^{zz} = -\frac{1}{2N} \sum_{\vec{p}} \frac{B_o}{A_o} \quad (16)$$

$$\delta m^{+-} = -\frac{1}{2N} \sum_{\vec{p}} \coth \frac{\beta E(\vec{p})}{2} \left[\Delta m_o \lambda \omega(\vec{p}) + \frac{1 - \frac{1}{2} \frac{\gamma_x(\vec{p}) + \gamma_y(\vec{p})}{6J}}{\omega(\vec{p})} \right] + \frac{1}{2} \coth \frac{\beta \lambda m_o}{2} (1 + \lambda \Delta m_o) \quad (17)$$

where:

$$A_o = 1 + \beta \lambda C_o \left(\gamma_x(\vec{p}) + \frac{\gamma_w^2(\vec{p})}{\gamma_x(\vec{p}) - 1} \right) \quad (18)$$

$$B_o = \beta \lambda \left(\gamma_x(\vec{p}) + \frac{\gamma_w^2(\vec{p})}{\gamma_x(\vec{p}) - 1} D_o + \frac{\gamma_w^2(\vec{p})}{(\gamma_x(\vec{p}) - 1)^2} \frac{C_o}{m_o} \right) \quad (19)$$

C_o and D_o is given by:

$$C_o = -\frac{1}{4} (1 - m_o^2) \quad (20)$$

$$D_o = m_o \Delta m_o \quad (21)$$

$$\Delta m_o = -\frac{\beta C_o}{1 + \beta \lambda C_o} \quad (22)$$

The magnon energy reads:

$$\begin{cases} E(\vec{p}) = \lambda m_o \omega(\vec{p}) \\ \omega^2(\vec{p}) = (1 - \gamma_x(\vec{p})) (1 - \gamma_y(\vec{p})) \end{cases} \quad (23)$$

Note that in the equations (16), (17) and in the following the sums run over the whole Brillouin zone. The contributions of the longitudinal and transverse fluctuations to the free per site are given by:

$$\delta F_{zz} = \frac{1}{2\beta} \sum_{\vec{p}} \ln A_o \quad (24)$$

$$\delta F_{+-} = \frac{1}{\beta} \sum_{\vec{p}} \ln \frac{\text{sh} \frac{\beta E(\vec{p})}{2}}{\text{sh} \frac{\beta \lambda m_o}{2}} \quad (25)$$

Where the single occupancy condition is disregarded, on the equations from (23) to (25) the following replacement should be done:

$$m_o \rightarrow \tilde{m}_o \quad (26)$$

It is easy to check that at zero temperature limit it does not matter whether the constraint is treated exactly or on the average the magnetization and the free energy are the same for both cases of the constraint conditions. Taking the limit of zero temperature $T \rightarrow 0K$ for the above equation we get the same sublattice magnetization and the ground state energy obtained in linear spin wave approximation by mean of Holstein- Primakov representation [12-15].

On the contrary, at finite temperature the exact constraint lead to the different values of the thermodynamical quantities, e.g., the magnetization, the internal energy, the specific heat... Fig 4 and Fig 5 show the difference in the finite temperature properties of the two methods of treating the constraint conditions for both ordered states.

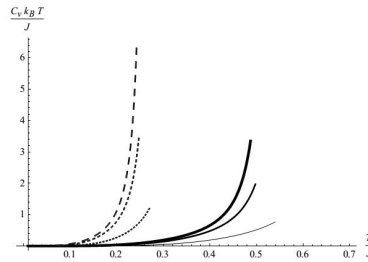


Figure 4. Temperature dependence of specific heat (for exact constraint: full line, from right to left and for average constraint: dashed line, from right to left) for collinear phase with $\alpha = 0, \alpha = 0.4, \alpha = 0.5$.

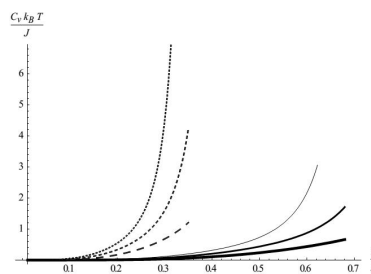


Figure 5. Temperature dependence of specific heat (for exact constraint: full line, from left to right and for average constraint: dashed line, from left to right) for incommensurate spiral phase with $\alpha = 0.75, \alpha = 1, \alpha = 2$.

4. Conclusion

We get the ground state properties of the spatially anisotropic triangular magnets consistent with the results obtained by mean of other linear spin wave theories [12-15]. This confirms the fact that at the zero temperature the Popov-Fedotov approach does not improve the results when the constraint on slave particle is treated approximately.

At the finite temperatures the exact projection onto physical Hilbert space gives significant differences in comparison with average projection. This is due to thermal fluctuation of slave fermions into unphysical spinless state. At the parameter range of interest, our results agree with results of numerical investigations [16, 17].

It would be interesting to see how to extend the method used here to study the spin-liquid region and for spin quantum number $S > 1/2$.

Acknowledgment

This work was financially supported by the National Foundation for Science and Technology Development (NAFOSTED) of Vietnam under Grant No 103.01- 2014.23.

References

- [1] Richter J, Schalenburg J, and Honecker A 2004, in *"Quantum magnetism"*, Lecture notes in Physics 645, ed. by Schollwork U, Richter J, Farnell D J J and Bishop R F, Springer, Berlin, p.85
- [2] Misguich G and Lhuillier C 2004, in *Frustrated Spin Systems*, ed. by H. T. Diep, World Scientific Singapore, p. 299
- [3] Jolicœur Th and Le Guillou J C 1989, *Phys. Rev. B* **40** 2727
- [4] Chernyshev A L and Zhitomirsky M E 2009, *Phys. Rev. B* **79** 144416
- [5] Bernu B, Lecheminant P, Lhuillier C and Pierre L 1994, *Phys. Rev. B* **50** 10048
- [6] Wite S R and Chernyshev A L 2007, *Phys. Rev. Lett.* **99** 127004

- [7] Kulagin S A, Prokof'ev N, Starykh O A, Svistunov B and Varney C N 2013, *Phys. Rev. B* **87** 024407
- [8] Nakatsuji S, Nambu Y, and Onada S 2010, *J. Phys. Soc. Jpn.* **79** 01103
- [9] Coldea R, Tennant D A, and Tylczynski Z 2003, *Phys. Rev. B* **68** 13442
- [10] Zvyagin S et al 2014, *Phys. Rev. Lett.* **112** 077206
- [11] Ono T et al 2003, *Phys. Rev. B* **67** 104431
- [12] Trumper A E 1999, *Phys. Rev. B* **60** 2987
- [13] Morino J, McKenzie R H, Marston J B and Chung C H 1999, *J. Phys: Condens. Matter*, **11** 2965
- [14] Bhaumik U and Taraphder A 2006, *J. Phys. Condens. Matter*, **18** 8251
- [15] Schmidt B and Thalmeier P 2014, *Phys. Rev. B* **89** 184402
- [16] Zheng W, Singh R R P, McKenzie R H and Coldea R 2005, *Phys. Rev. B* **71** 134422
- [17] Bishop R F, Li P H Y, Farrell D J J, Campell C F 2009, *Phys. Rev. B* **79** 174405
- [18] Popov V N and Fedotov S A 1988, *Sov. Phys. JETP* **67** 535
- [19] Veits O et al 1994, *J. France* **4** 493
- [20] Tejima S and Oguchi A 1995, *J. Phys. Soc. Jpn.* **64** 4923
- [21] Azakov S, Dilaver M and Oztas 2000, *Int. J. Mod. Phys. B* **14** 13
- [22] Dillenschneider R and Richert J 2006, *Eur. Phys. J. B* **49** 187
- [23] Kicelev M N, Feldmann H and Opperman R 2002, *Phys. Rev. B* **65** 184410
- [24] Kicelev M N 2006, *Int. J. Mod. Phys. B* **20**, 381.
- [25] Pham Thi Thanh Nga and Nguyen Toan Thang 2012, *Comm. in Phys.* **22** 33; *Comm. in Phys.* **22** 383
Erratum.